Formation of a G-Quartet-Fe Complex and Modulation of Electronic and Magnetic Properties of the Fe Center

Likun Wang,[†] Huihui Kong,[†] Chi Zhang,[†] Qiang Sun,[†] Liangliang Cai,[†] Qinggang Tan,[†] Flemming Besenbacher,[‡] and Wei Xu*[,†]

[†]Tongji-Aarhus Joint Research Center for Nanostructures and Functional Nanomaterials and College of Materials Science and Engineering, Tongji University, Caoan Road 4800, Shanghai 201804, People's Republic of China and [‡]Interdisciplinary Nanoscience Center (iNANO) and Department of Physics and Astronomy, Aarhus University, DK-8000 Aarhus C, Denmark

ABSTRACT Although the G-quartet structure has been extensively investigated due to its biological importance, the formation mechanism, in particular, the necessity of metal centers, of an isolated G-quartet on solid surfaces remains ambiguous. Here, by using scanning tunneling microscopy under well-controlled ultra-high-vacuum conditions and density functional theory calculations we have been able to clarify that besides the intraquartet hydrogen bonding a metal center is mandatory for the formation of an isolated G-quartet. Furthermore, by subtly perturbing the local coordination bonding schemes within the formed G-quartet complex *via* local nanoscale scanning tunneling microscopy manipulations, we succeed in modulating the d orbitals and the accompanying magnetic properties of the metal center. Our results demonstrate the feasibility of forming an isolated G-quartet complex on a solid surface and that the strategy of modulating electronic and magnetic properties of the metal center can be extended to other related systems such as molecular spintronics.

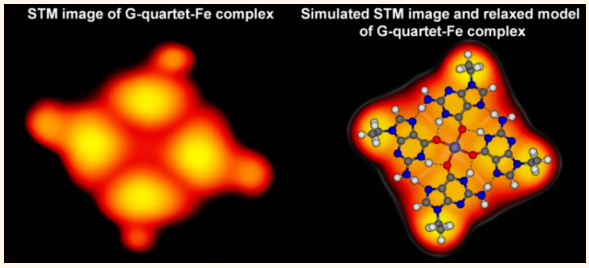

KEYWORDS: scanning tunneling microscopy · G-quartet · density functional theory · coordination bond · nanoscale manipulation

Ever since its identification in 1962,[1] the guanine quartet (G-quartet) structure has attracted enormous attention in many different fields ranging from structural biology to biochemistry and recently to surface physical chemistry.[2−6] The G-quartet is a planar macrocycle formed by four Hoogsteen paired G molecules, and in a cellular environment, G-quartets can stack on top of each other with template cations in between to form the so-called G-quadruplex, which has proven to be crucial for several biological processes.[3,4,7−10] Recently, it has been shown that the G-quardruplex can be stabilized by small molecules and then visualized in human cells.[4,9] In liquid or at solid−liquid interfaces, metal cations are usually needed to stabilize the G-quartet structures.[6,11−14] Some conformationally constrained G analogues can also self-assemble into empty G-quartets due to steric hindrance.[15−17] On solid surfaces, it has been shown that empty G-quartet network structures can be self-assembled on Au(111) by unfunctionalized G molecules,[18,19] and later on these network structures were used as templates to investigate the interactions between G molecules and potassium atoms.[20,21] As a simple model system, however, an isolated G-quartet structure without additional large functional groups is yet to be formed on solid surfaces under ultra-high-vacuum (UHV) conditions, which would allow for the atomic-scale real-space investigation of the fundamental interactions and intrinsic properties in the absence of disturbing factors. More importantly, it is even still ambiguous whether metal centers are needed in such a formation process. It is therefore of great interest to explore if and how an isolated G-quartet structure can be formed on surfaces under UHV conditions to reveal the detailed formation mechanism and moreover to investigate the fundamental interactions and physical and chemical properties of such a biologically relevant model system at the atomic scale.

In this work, a 9-ethylguanine (9eG) molecule is chosen for the purpose of structural

* Address correspondence to xuwei@tongji.edu.cn.

Received for review September 24, 2014 and accepted October 27, 2014.

Published online October 27, 2014
10.1021/nn5054156

mimics of a natural G nucleoside; also, the ethyl group screens the possible interquartet hydrogen bonding.[18,19] The Fe atom, as a typical magnetic transition metal,[22−26] is found to preferentially coordinate with an O atom;[27] thus, it is chosen here as a control parameter to probe its necessity in the formation of an isolated G-quartet structure. Herein, from an interplay of high-resolution scanning tunneling microscopy (STM) imaging and lateral STM manipulations combined with density functional theory (DFT) calculations, we show that (1) 9eG molecules self-assemble into the well-known G ribbon structure (as depicted in the upper panel of Figure 1)[11,28−30] rather than the G-quartet structure on Au(111). (2) Interestingly, simultaneous co-deposition of 9eG molecules and Fe atoms results in the formation of isolated G-quartet-Fe complexes (as depicted in the lower panel of Scheme 1). Local density of states (LDOS) and charge density difference analyses illustrate that the driving forces behind the formation of such a complex is the cooperative effect of coordination bonding and intraquartet hydrogen bonding. (3) Projected density of states (PDOS) and spin density analyses further demonstrate that both adsorption and coordination behaviors on the Au(111) surface result in the increase of the spin magnetic moment of the Fe center. (4) Further STM manipulations enable us to gradually decouple the interactions between the Fe atom and 9eG molecules within the formed G-quartet-Fe complex, leading to the success of modulating the d orbitals and the accompanying magnetic properties of the Fe center. These findings thus unravel the formation mechanism of the G-quartet-Fe complex on the inert Au(111) surface, and in particular, lateral STM manipulation provides us a unique approach to delicately modulate the electronic and magnetic properties of a metallic center in metal−organic complexes.

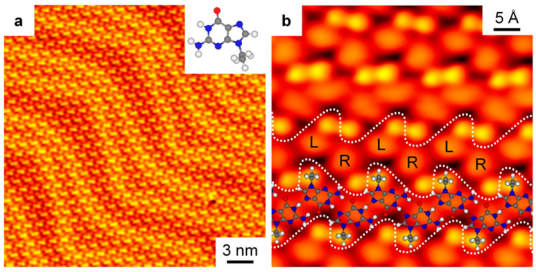

Figure 1. Self-assembled G ribbon structure formed by 9eG molecules on Au(111). (a) Large-scale STM image shows the formation of a G ribbon structure (scanning conditions: I_t = 0.86 nA, V_t = −1.77 V). The inset shows the chemical structure of the 9eG molecule. (b) Close-up STM image allows us to distinguish the submolecularly resolved topography of individual molecule and molecular chiralities (as indicated in the image by the R and L notation) (scanning conditions: I_t = 0.64 nA, V_t = −1.25 V). The dashed wavy lines separate the adjacent antiparallel ribbons. The DFT-optimized structural model is superimposed on one of the ribbons, where a good agreement is achieved.

RESULTS AND DISCUSSION

After the deposition of 9eG molecules on Au(111), a well-ordered molecular nanostructure is observed as depicted in Figure 1a. The close-up STM image (Figure 1b) reveals that the nanostructure is formed by laterally connected zigzag ribbons indicated by the dashed wavy lines. The single molecule is imaged as a relatively dark protrusion and a bright round protrusion, which are assigned to the guanine moiety and the tilted ethyl group, respectively.[28] From the submolecularly resolved STM topography of individual molecules we can thus distinguish the molecular chiralities as indicated by R and L in Figure 1b. Hence, we can identify that each ribbon is formed by alternating R and L chiral forms, and the adjacent ribbons are antiparallel with respect to each other. On the basis of our experimental observations we have built up the structural models and relaxed them by DFT methods, and the most stable one is overlaid on

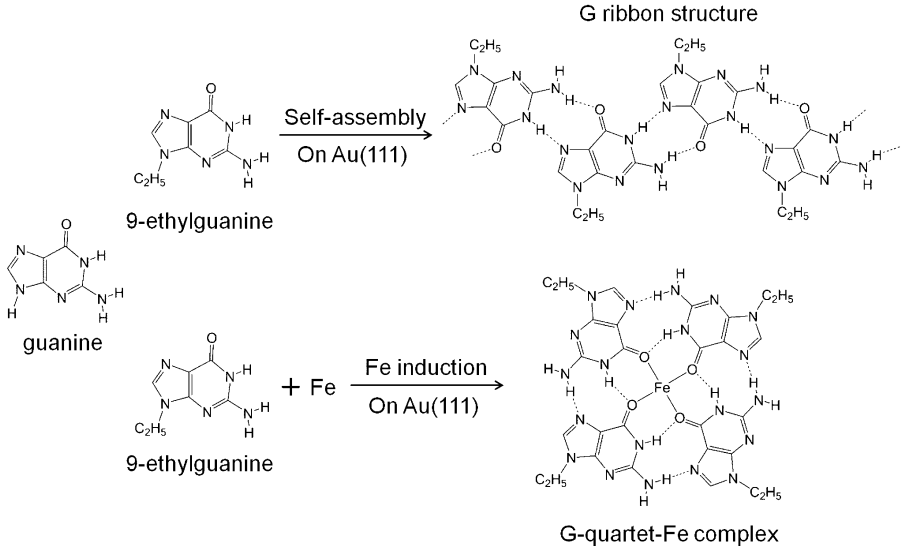

Scheme 1. Schematic Illustration of the Formation of the G Ribbon Structure and G-Quartet-Fe Complex on Au(111)

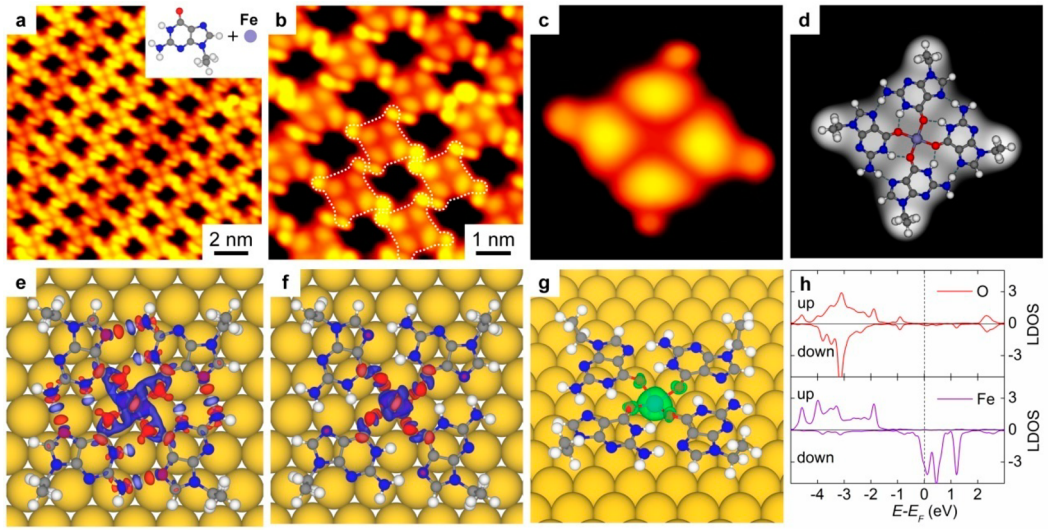

Figure 2. Formation of G-quartet-Fe complex on Au(111). (a) Large-scale STM image shows the formation of a close-packed structure of the G-quartet-Fe complex (scanning conditions: $I_t = 0.85$ nA, $V_t = 1.77$ V). The inset shows the chemical structure of a 9eG molecule and an Fe atom. (b) Close-up STM image showing the details of the structure where four individual G-quartet-Fe complexes are depicted by the dashed contours. (c) Submolecularly resolved STM image of an isolated G-quartet-Fe complex. (d) Simulated STM image of the complex with the DFT-optimized structural model superimposed. Blue dashed lines represent hydrogen bonds. (e and f) Charge density difference maps of the complex showing the hydrogen bonding and coordination bonding, where red and blue isosurfaces indicate charge accumulation and depletion, respectively (four 9eG molecules are considered to be four individual species and a whole in e and f, respectively). (g) Perspective view of the spin density distribution of the complex. (h) Upper and lower panels show LDOS (in [eV] with respect to the Fermi energy E_F) of O atoms (sum of four O atoms) and Fe atom in the optimized model, respectively.

top of the STM image, where good agreement is achieved as depicted in Figure 1b. As seen from the model, we could identify that along the ribbons each molecule binds to the other two *via* double hydrogen bonds (N−H···N and N−H···O),[6] and between the ribbons, molecules interact with each other *via* van der Waals (vdW) forces from the tilted ethyl groups.

Note that, according to previous work, the G molecules self-assemble into an empty G-quartet network structure on Au(111).[18] We would thus naturally anticipate the formation of an isolated G-quartet structure by deposition of 9eG molecules on the same surface, in which the intraquartet hydrogen bonding should be exactly the same as the one in the original G-quartet structure[18] and the ethyl groups screen the interquartet hydrogen bonding. In our experiments, however, only a G ribbon structure is observed at various coverages. To unravel the reason behind this discrepancy, we have performed DFT-D2 calculations on the binding energy of each structure (see Supporting Information, Figure 1). In comparison with the isolated G-quartet structure, the G ribbon structure is energetically more favorable by 0.17 eV per molecule. Consequently, it appears that the intraquartet hydrogen bonding alone is not sufficient for the formation of a G-quartet structure, and then the resonance-assisted hydrogen bonding (RAHB) effect described previously[18] might need to be revisited.[31] Thus, without the energy gain from interquartet hydrogen bonding the 9eG molecules prefer to form the G ribbon structure rather than the G-quartet structure on Au(111).

To explore the possibility of forming an isolated G-quartet structure on the Au(111) surface under UHV conditions, we perform further experiments by simultaneous co-deposition of 9eG molecules and Fe atoms onto the surface. Interestingly, such co-deposition leads to the formation of well-ordered G-quartet-Fe complex arrays as shown in Figure 2a. At low doses of Fe atoms, discrete G-quartet-Fe complexes are found to coexist with the G ribbon structure mentioned above (see Supporting Information Figure 2), and these two intrinsically different nanostructures are sensitively dependent on the doses of Fe atoms.[32] Close-up STM image (Figure 2b) allows us to observe the details of the structure where four adjacent G-quartet-Fe complexes are depicted by the dashed contours and each one is packed with four other neighbors by vdW interactions from the ethyl groups. To get a deeper insight into the intrinsic properties of the G-quartet-Fe complex, we obtain a submolecularly resolved STM image of an isolated complex (Figure 2c) from a low-coverage sample. Note that the ethyl groups in an isolated complex appear smaller than the ones in the close-packed arrays (Figure 2b), which is most likely due to their flexibility (*i.e.*, either tilted in the close-packed arrays or relatively flat in an isolated one). It should also be noted that the Fe center in the complex is usually not visible. Based on the high-resolution STM images, we have obtained the DFT-optimized energetically most favorable model of the G-quartet-Fe complex, which is overlaid on the corresponding simulated STM image as shown in

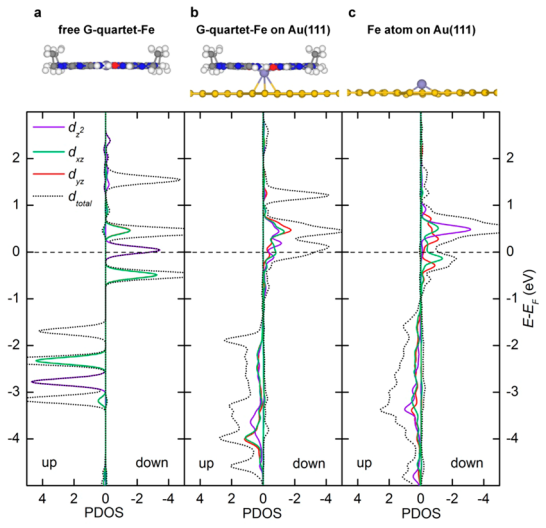

Figure 3. PDOS on the d_{z^2}, d_{xz}, d_{yz}, and d_{total} orbitals of (a) the Fe atom in the free G-quartet-Fe complex, (b) the Fe atom in the adsorbed G-quartet-Fe complex on Au(111), and (c) an isolated Fe atom on Au(111).

Figure 2d (the substrate included in the calculations has been cut out for clarity). On the basis of the optimized model, we perform further DFT calculations on the electronic and magnetic properties of the G-quartet-Fe complex. From charge density difference maps (Figure 2e,f) we identify that the Fe center coordinates with the four O atoms of 9eG molecules, and four 9eG molecules form intraquartet hydrogen bonding similar to that in the original G-quartet structure.[18] The coordination bonding between the O atom and Fe atom can be further illustrated by LDOS of the two elements shown in Figure 2h, in which several hybridization peaks can be observed below the Fermi energy. Hence, the formation of the G-quartet-Fe complex is attributed to the cooperative effect of intraquartet hydrogen bonding and coordination bonding. LDOS of the Fe atom also displays a large splitting between the spin-up and spin-down states (Figure 2h). As a result, the Fe center is strongly magnetized with a total magnetic moment calculated to be 3.63 μ_B, indicating a high-spin electronic configuration. The corresponding spin density distribution of the complex is also shown in Figure 2g. It is worth noting that each O atom in the complex also exhibits a small magnetic moment of about 0.04 μ_B induced by the Fe center.

To get further insight into the effect of adsorption and coordination behaviors on the electronic and magnetic properties of the Fe center, we perform systematic calculations on the PDOS on different d orbitals of the Fe atom in various environments as shown in Figure 3a–c. Upon adsorption of the G-quartet-Fe complex on Au(111), the broadened d_π (*i.e.*, d_{xz} and d_{yz}) and d_{z^2} orbitals show an apparent hybridization between the Fe atom and the substrate (compare Figure 4a and b). Interestingly, the energy interval in Figure 3a (from −1.70 to −0.49 eV) between the spin-up and spin-down d_{total} orbital increases by about 0.78 eV (Figure 3b), and as a result, the magnetic moment of the Fe center increases from 3.14 μ_B to 3.63 μ_B upon adsorption on Au(111). On the other hand, the magnetic moment of an isolated Fe atom on Au(111) is calculated to be 3.27 μ_B, which means that coordination with O atoms within the G-quartet-Fe complex on Au(111) leads to an increase in the magnetic moment.[23] It is worth noting that a small difference is observed for the d_π orbitals of the Fe atom in a free complex (Figure 3a) and on the surface (Figure 3b,c). The peaks of the d_π orbitals of the Fe atom in the free complex overlap each other, whereas they are separated both in the on-surface complex and for the isolated one. The difference in the d_π orbitals originates from the local symmetry of the adsorption site, which is similar to the lift of degeneracy in d_π orbitals of a bridge-site-adsorbed FePc molecule on Au(111).[33]

Going a step further, modulation of electronic and magnetic properties of the Fe center would be of utmost interest to explore, and naturally, a direct way would be to locally perturb the coordination bonding scheme between the metal center and the molecules.[34] In fact, STM manipulations have previously been employed on TBrPP-Co or CoPc molecules to either change the two-dimensional self-assembly[35] or break the peripheral chemical bonding of a single molecule[36] with the success of controlling electronic and magnetic properties of the metal centers. Due to the rigidity of TBrPP-Co and CoPc molecules, however, directly changing the coordination bonding scheme within a single molecule remains difficult. In this aspect, the relatively flexible G-quartet-Fe complex consequently renders the possibility to change the coordination bonding scheme and furthermore to probe the electronic and magnetic properties of the Fe center in different bonding configurations. Experimentally, we indeed succeed in constructing another two transformed configurations of the G-quartet-Fe complex *via* lateral STM manipulations (Figure 4b,c), which are similar to the theoretical models proposed previously.[37] In comparison to the original G-quartet-Fe complex (Figure 4a) one of the 9eG molecules (indicated by the white arrow) is rotated counterclockwise with an angle of about 50° (Figure 4b), and subsequently, another molecule (indicated by the white arrow) has undergone the same rotation (Figure 4c). From the DFT relaxed models we identify that such manipulations indeed result in local perturbations on the coordination bonding scheme within the G-quartet-Fe complex where the interactions between the Fe center and 9eG molecules are gradually decoupled (Figure 4d–f). From the side view of the models we can also see that the Fe atom adsorbs closer and closer to the substrate as the decoupling with the molecules proceeds. Interestingly, in the configuration in Figure 4c the previously invisible Fe center can now be visualized as a dim protrusion, indicating the change in the electronic

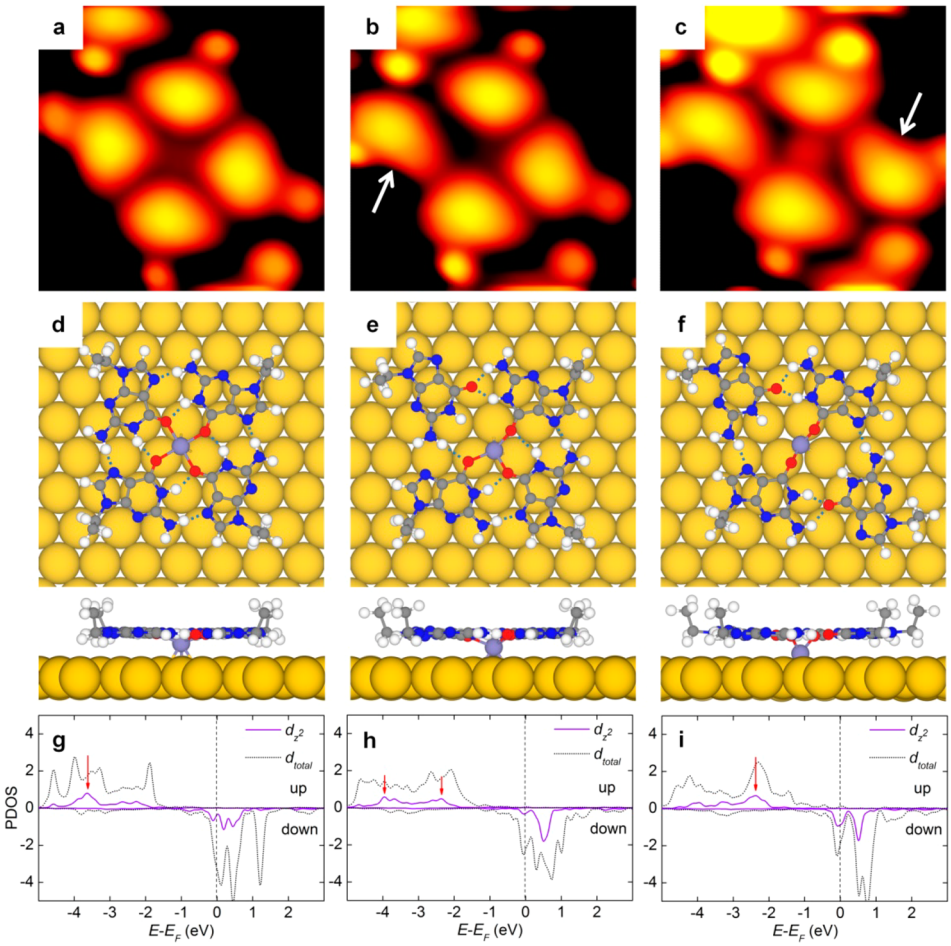

Figure 4. Modulation of the d band structure of the Fe center. (a−c) Series of STM images showing the subtle structural change of the G-quartet-Fe complex induced by lateral STM manipulations. In particular, the Fe center starts showing the electronic density of states and can be visualized as a dim protrusion in the structure shown in c. (d−f) Corresponding DFT-optimized structural models of the ones shown in a−c. Side views show that the Fe center gradually moves downward to the substrate as the decoupling with the molecules proceeds. (g−i) Corresponding PDOS on the d_{z^2} and d_{total} orbitals of the Fe center in these three different structures. The vertical red arrows indicate that the main peak of the d_{z^2} orbital in the spin-up state moves toward the Fermi energy as the decoupling proceeds.

density of states of the Fe center. To unravel the change of electronic and magnetic properties of the Fe center in different bonding configurations, we again perform PDOS calculations based on the optimized models as shown in Figure 4g−i. As indicated by the red arrows, we can clearly identify that the main peak of the d_{z^2} orbital in the spin-up states moves gradually toward the Fermi energy (the d_{total} orbital shows the same tendency). Also, the spin splitting of the orbitals of the Fe atom is reduced along with the decoupling process, and as a result, the magnetic moment of the Fe atom decreases from 3.63 μ_B to 3.53 μ_B to 3.36 μ_B in configurations in Figure 4d, e, and f, respectively. Thus, we have successfully modulated the d orbitals and the accompanying magnetic properties of the Fe center within the G-quartet-Fe complex by directly perturbing the local bonding scheme with lateral STM manipulations.

CONCLUSIONS

These findings give us further insight into the formation mechanism of an isolated G-quartet structure in which besides the intraquartet hydrogen bonding a metal center capable of coordinating with O atoms is mandatory. We propose that the strategy presented in this work, that is, modulation of the electronic and magnetic properties of the metal center by subtly perturbing the local bonding schemes with STM manipulations, can be extended to other related systems and warrants further studies such as molecular spintronics.

METHODS

All STM experiments were performed in a UHV chamber (base pressure 1 × 10^{-10} mbar) equipped with variable-temperature, fast-scanning "Aarhus-type" STM,[38,39] a molecular evaporator, and an e-beam evaporator, and other standard instrumentation for sample preparation. The Au(111) substrate was prepared by

several cycles of 1.5 keV Ar^+ sputtering followed by annealing to 770 K for 15 min, resulting in clean and flat terraces separated by monatomic steps. The 9eG molecules were loaded into a glass crucible in the molecular evaporator. After a thorough degassing, the molecules were deposited onto the clean substrate by thermal sublimation at 440 K; the Fe atoms were simultaneously deposited onto the surfaces at RT. After preparation, the samples were imaged by STM over a temperature range of 100−150 K. The lateral manipulations[40] were carried out by consecutively scanning on a close-up G-quartet-Fe complex for the purpose of perturbing the ethyl groups, which successfully resulted in the manipulation of the 9eG molecules.

The calculations were performed in the framework of DFT by using the Vienna *ab initio* simulation package (VASP).[41,42] The projector-augmented wave method was used to describe the interaction between ions and electrons; the Perdew−Burke−Ernzerhof generalized gradient approximation (GGA) exchange−correlation functional was employed,[43] and van der Waals interactions were included using the dispersion-corrected DFT-D2 method of Grimme[44] for the calculations when including the gold surface. The atomic structures were relaxed using the conjugate gradient algorithm scheme as implemented in the VASP code until the forces on all unconstrained atoms were ≤0.03 eV/Å. The simulated STM images were obtained by the Hive program based on the Tersoff−Hamann method.[45,46]

Conflict of Interest: The authors declare no competing financial interest.

Supporting Information Available: DFT-calculated structural models of G ribbon structure and G-quartet structure and the respective energy values, coexistence of the G-quartet complex and the G ribbon structure at low doses of Fe atoms, comparison of the simplified G-quartet network formed by canonical guanine molecules with G-quartet-Fe complex arrays formed by 9-ethylguanine molecules and Fe atoms. This material is available free of charge *via* the Internet at http://pubs.acs.org.

Acknowledgment. Prof. Lev Kantorovich is greatly acknowledged for fruitful discussions about the manuscript. The authors acknowledge financial support from the National Natural Science Foundation of China (21103128, 21473123), the Shanghai "Shu Guang" project supported by the Shanghai Municipal Education Commission and Shanghai Education Development Foundation (11SG25), and the Research Fund for the Doctoral Program of Higher Education of China (20120072110045).

REFERENCES AND NOTES

1. Gellert, M.; Lipsett, M. N.; Davies, D. R. Helix Formation by Guanylic Acid. *Proc. Natl. Acad. Sci. U.S.A.* **1962**, *48*, 2013–2018.
2. Davis, J. T. G-Quartets 40 Years Later: From 5′-GMP to Molecular Biology and Supramolecular Chemistry. *Angew. Chem., Int. Ed.* **2004**, *43*, 668–698.
3. Williamson, J. R. G-Quartet Structures in Telomeric DNA. *Annu. Rev. Biophys. Biomol. Struct.* **1994**, *23*, 703–730.
4. Biffi, G.; Di Antonio, M.; Tannahill, D.; Balasubramanian, S. Visualization and Selective Chemical Targeting of RNA G-Quadruplex Structures in the Cytoplasm of Human Cells. *Nat. Chem.* **2014**, *6*, 75–80.
5. Masiero, S.; Gottarelli, G.; Pieraccini, S. G-Quartets as a Self-Assembled Scaffold for Circular Porphyrin Arrays. *Chem. Commun.* **2000**, 1995–1996.
6. Ciesielski, A.; Lena, S.; Masiero, S.; Spada, G. P.; Samori, P. Dynamers at the Solid-Liquid Interface: Controlling the Reversible Assembly/Reassembly Process between Two Highly Ordered Supramolecular Guanine Motifs. *Angew. Chem., Int. Ed.* **2010**, *49*, 1963–1966.
7. McLuckie, K. I.; Di Antonio, M.; Zecchini, H.; Xian, J.; Caldas, C.; Krippendorff, B. F.; Tannahill, D.; Lowe, C.; Balasubramanian, S. G-Quadruplex DNA as a Molecular Target for Induced Synthetic Lethality in Cancer Cells. *J. Am. Chem. Soc.* **2013**, *135*, 9640–9643.
8. Kumari, S.; Bugaut, A.; Huppert, J. L.; Balasubramanian, S. An RNA G-Quadruplex in the 5′ UTR of the *NRAS* Proto-Oncogene Modulates Translation. *Nat. Chem. Biol.* **2007**, *3*, 218–221.
9. Biffi, G.; Tannahill, D.; McCafferty, J.; Balasubramanian, S. Quantitative Visualization of DNA G-Quadruplex Structures in Human Cells. *Nat. Chem.* **2013**, *5*, 182–186.
10. Bochman, M. L.; Paeschke, K.; Zakian, V. A. DNA Secondary Structures: Stability and Function of G-Quadruplex Structures. *Nat. Rev. Genet.* **2012**, *13*, 770–780.
11. Kwan, I. C.; Mo, X.; Wu, G. Probing Hydrogen Bonding and Ion-Carbonyl Interactions by Solid-State ^{17}O NMR Spectroscopy: G-Ribbon and G-Quartet. *J. Am. Chem. Soc.* **2007**, *129*, 2398–2407.
12. Engelhard, D. M.; Pievo, R.; Clever, G. H. Reversible Stabilization of Transition-Metal-Binding DNA G-Quadruplexes. *Angew. Chem., Int. Ed.* **2013**, *52*, 12843–12847.
13. Kwan, I. C. M.; Wong, A.; She, Y.-M.; Smith, M. E.; Wu, G. Direct NMR Evidence for Ca^{2+} Ion Binding to G-Quartets. *Chem. Commun.* **2008**, 682–684.
14. Ida, R.; Wu, G. Direct NMR Detection of Alkali Metal Ions Bound to G-Quadruplex DNA. *J. Am. Chem. Soc.* **2008**, *130*, 3590–3602.
15. Sessler, J. L.; Sathiosatham, M.; Doerr, K.; Lynch, V.; Abboud, K. A. A G-Quartet Formed in the Absence of a Templating Metal Cation: A New 8-(N,N-Dimethylaniline) Guanosine Derivative. *Angew. Chem., Int. Ed.* **2000**, *112*, 1356–1359.
16. Pham, T. N.; Masiero, S.; Gottarelli, G.; Brown, S. P. Identification by ^{15}N Refocused INADEQUATE MAS NMR of Intermolecular Hydrogen Bonding That Directs the Self-Assembly of Modified DNA Bases. *J. Am. Chem. Soc.* **2005**, *127*, 16018–16019.
17. González-Rodríguez, D.; Janssen, P. G.; Martín-Rapún, R.; Cat, I. D.; Feyter, S. D.; Schenning, A. P.; Meijer, E. W. Persistent, Well-Defined, Monodisperse, π-Conjugated Organic Nanoparticles *via* G-Quadruplex Self-Assembly. *J. Am. Chem. Soc.* **2009**, *132*, 4710–4719.
18. Otero, R.; Schöck, M.; Molina, L. M.; Lægsgaard, E.; Stensgaard, I.; Hammer, B.; Besenbacher, F. Guanine Quartet Networks Stabilized by Cooperative Hydrogen Bonds. *Angew. Chem., Int. Ed.* **2005**, *44*, 2270–2275.
19. Xu, W.; Kelly, R. E.; Gersen, H.; Lægsgaard, E.; Stensgaard, I.; Kantorovich, L. N.; Besenbacher, F. Prochiral Guanine Adsorption on Au(111): An Entropy-Stabilized Intermixed Guanine-Quartet Chiral Structure. *Small* **2009**, *5*, 1952–1956.
20. Xu, W.; Tan, Q.; Yu, M.; Sun, Q.; Kong, H.; Lægsgaard, E.; Stensgaard, I.; Kjems, J.; Wang, J.; Wang, C.; *et al*. Atomic-Scale Structures and Interactions Between the Guanine Quartet and Potassium. *Chem. Commun.* **2013**, *49*, 7210–7212.
21. Xu, W.; Wang, J. G.; Yu, M.; Lægsgaard, E.; Stensgaard, I.; Linderoth, T. R.; Hammer, B.; Wang, C.; Besenbacher, F. Guanine- and Potassium-Based Two-Dimensional Coordination Network Self-Assembled on Au(111). *J. Am. Chem. Soc.* **2010**, *132*, 15927–15929.
22. Messina, P.; Dmitriev, A.; Spillmann, H.; Abel, M.; Barth, J. V.; Kern, K. Direct Observation of Chiral Metal-Organic Complexes Assembled on a Cu(100) Surface. *J. Am. Chem. Soc.* **2002**, *124*, 14000–14001.
23. Classen, T.; Fratesi, G.; Costantini, G.; Fabris, S.; Stadler, F. L.; Kim, C.; Gironcoli, S.; Baroni, S.; Kern, K. Templated Growth of Metal-Organic Coordination Chains at Surfaces. *Angew. Chem., Int. Ed.* **2005**, *44*, 6142–6145.
24. Tait, S. L.; Wang, Y.; Costantini, G.; Lin, N.; Baraldi, A.; Esch, F.; Petaccia, L.; Lizzit, S.; Kern, K. Metal-Organic Coordination Interactions in Fe-Terephthalic Acid Networks on Cu(100). *J. Am. Chem. Soc.* **2008**, *130*, 2108–2113.
25. Gambardella, P.; Stepanow, S.; Dmitriev, A.; Honolka, J.; Groot, F. M. F.; Lingenfelder, M.; Gupta, S. S.; Sarma, D. D.; Bencok, P.; Stanescu, S.; *et al*. Supramolecular Control of the Magnetic Anisotropy in Two-Dimensional High-Spin Fe Arrays at a Metal Interface. *Nat. Mater.* **2009**, *8*, 189–193.
26. Cechal, J.; Kley, C. S.; Kumagai, T.; Schramm, F.; Ruben, M.; Stepanow, S.; Kern, K. Functionalization of Open Two-Dimensional Metal-Organic Templates Through the Selective Incorporation of Metal Atoms. *J. Phys. Chem. C* **2013**, *117*, 8871–8877.

27. Langner, A.; Tait, S. L.; Lin, N.; Chandrasekar, R.; Meded, V.; Fink, K.; Ruben, M.; Kern, K. Selective Coordination Bonding in Metallo-Supramolecular Systems on Surfaces. *Angew. Chem., Int. Ed.* **2012**, *51*, 4327–4331.
28. Xu, W.; Wang, J.; Jacobsen, M. F.; Mura, M.; Yu, M.; Kelly, R. E. A.; Meng, Q.; Lægsgaard, E.; Stensgaard, I.; Linderoth, T. R.; *et al*. Supramolecular Porous Network Formed by Molecular Recognition between Chemically Modified Nucleobases Guanine and Cytosine. *Angew. Chem., Int. Ed.* **2010**, *49*, 9373–9377.
29. Ciesielski, A.; Perone, R.; Pieraccini, S.; Spada, G. P.; Samori, P. Nanopatterning the Surface with Ordered Supramolecular Architectures of N^9-Alkylated Guanines: STM Reveals. *Chem. Commun.* **2010**, *46*, 4493–4495.
30. Webber, A. L.; Masiero, S.; Pieraccini, S.; Burley, J. C.; Tatton, A. S.; Iuga, D.; Pham, T. N.; Spada, G. P.; Brown, S. P. Identifying Guanosine Self Assembly at Natural Isotopic Abundance by High-Resolution ^{1}H and ^{13}C Solid-State NMR Spectroscopy. *J. Am. Chem. Soc.* **2011**, *133*, 19777–19795.
31. Guerra, C.; Zijlstra, H.; Paragi, G.; Bickelhaupt, F. M. Telomere Structure and Stability: Covalency in Hydrogen Bonds, Not Resonance Assistance, Causes Cooperativity in Guanine Quartets. *Chem.—Eur. J.* **2011**, *17*, 12612–12622.
32. Tseng, T. C.; Abdurakhmanova, N.; Stepanow, S.; Kern, K. Hierarchical Assembly and Reticulation of Two-Dimensional Mn- And Ni-$TCNQ_X$ (X = 1, 2, 4) Coordination Structures on a Metal Surface. *J. Phys. Chem. C* **2011**, *115*, 10211–10217.
33. Minamitani, E.; Tsukahara, N.; Matsunaka, D.; Kim, Y.; Takagi, N.; Kawai, M. Symmetry-Driven Novel Kondo Effect in a Molecule. *Phys. Rev. Lett.* **2012**, *109*, 086602.
34. Urgel, J. I.; Ecija, D.; Auwärter, W.; Barth, J. V. Controlled Manipulation of Gadolinium-Coordinated Supramolecules by Low-Temperature Scanning Tunneling Microscopy. *Nano Lett.* **2014**, *14*, 1369–1373.
35. Iancu, V.; Deshpande, A.; Hla, S.-W. Manipulation of the Kondo Effect *via* Two-Dimensional Molecular Assembly. *Phys. Rev. Lett.* **2006**, *97*, 266603.
36. Zhao, A.; Li, Q.; Chen, L.; Xiang, H.; Wang, W.; Pan, S.; Wang, B.; Xiao, X.; Yang, J.; Hou, J. G.; *et al*. Controlling the Kondo Effect of an Adsorbed Magnetic Ion through Its Chemical Bonding. *Science* **2005**, *309*, 1542–1544.
37. Livshits, A. I.; Kantorovich, L. Guanine Assemblies on the Au (111) Surface: A Theoretical Study. *J. Phys. Chem. C* **2013**, *117*, 5684–5692.
38. Besenbacher, F. Scanning Tunnelling Microscopy Studies of Metal Surfaces. *Rep. Prog. Phys.* **1996**, *59*, 1737–1802.
39. Lægsgaard, E.; Österlund, L.; Thostrup, P.; Rasmussen, P. B.; Stensgaard, I.; Besenbacher, F. A High-Pressure Scanning Tunneling Microscope. *Rev. Sci. Instrum.* **2001**, *72*, 3537–3542.
40. Xu, W.; Kong, H.; Zhang, C.; Sun, Q.; Gersen, H.; Dong, L.; Tan, Q.; Lægsgaard, E.; Besenbacher, F. Identification of Molecular-Adsorption Geometries and Intermolecular Hydrogen-Bonding Configurations by *in Situ* STM Manipulation. *Angew. Chem., Int. Ed.* **2013**, *52*, 7442–7445.
41. Kresse, G.; Hafner, J. *Ab Initio* Molecular Dynamics for Open-Shell Transition Metals. *Phys. Rev. B* **1993**, *48*, 13115.
42. Kresse, G.; Furthmüller, J. Efficient Iterative Schemes for *ab Initio* Total-Energy Calculations Using a Plane-Wave Basis Set. *Phys. Rev. B* **1996**, *54*, 11169.
43. Perdew, J. P.; Burke, K.; Ernzerhof, M. Generalized Gradient Approximation Made Simple. *Phys. Rev. Lett.* **1996**, *77*, 3865.
44. Grimme, S. Semiempirical GGA-Type Density Functional Constructed with a Long-Range Dispersion Correction. *J. Comput. Chem.* **2006**, *27*, 1787–1799.
45. Tersoff, J.; Hamann, D. Theory of the Scanning Tunneling Microscope. *Phys. Rev. B* **1985**, *31*, 805–813.
46. Vanpoucke, D. E.; Brocks, G. Formation of Pt-Induced Ge Atomic Nanowires on Pt/Ge(001): A Density Functional Theory Study. *Phys. Rev. B* **2008**, *77*, 241308.